Journal of Controlled Release 236 (2016) 15–21

Contents lists available at ScienceDirect

Journal of Controlled Release

journal homepage: www.elsevier.com/locate/jconrel

Acoustic Cluster Therapy (ACT) enhances the therapeutic efficacy of paclitaxel and Abraxane® for treatment of human prostate adenocarcinoma in mice

Annemieke van Wamel [a,*], Per Christian Sontum [b], Andrew Healey [b], Svein Kvåle [b], Nigel Bush [c], Jeffrey Bamber [c], Catharina de Lange Davies [a]

[a] Dept. of Physics, NTNU, Norwegian University of Science and Technology, Trondheim, Norway
[b] Phoenix Solutions AS, Oslo, Norway
[c] Joint Dept. of Physics, Institute of Cancer Research and Royal Marsden NHS Foundation Trust, London, UK

ARTICLE INFO

Article history:
Received 2 May 2016
Received in revised form 7 June 2016
Accepted 9 June 2016
Available online 11 June 2016

Keywords:
Acoustic cluster therapy
Act
Targeted drug delivery
Abraxane®
Paclitaxel
PC-3 prostate adenocarcinoma
Pre-clinical

ABSTRACT

Acoustic cluster therapy (ACT) is a novel approach for ultrasound mediated, targeted drug delivery. In the current study, we have investigated ACT in combination with paclitaxel and Abraxane® for treatment of a subcutaneous human prostate adenocarcinoma (PC3) in mice. In combination with paclitaxel (12 mg/kg given *i.p.*), ACT induced a strong increase in therapeutic efficacy; 120 days after study start, 42% of the animals were in stable, complete remission vs. 0% for the paclitaxel only group and the median survival was increased by 86%. In combination with Abraxane® (12 mg paclitaxel/kg given *i.v.*), ACT induced a strong increase in the therapeutic efficacy; 60 days after study start 100% of the animals were in stable, remission vs. 0% for the Abraxane® only group, 120 days after study start 67% of the animals were in stable, complete remission vs. 0% for the Abraxane® only group. For the ACT + Abraxane group 100% of the animals were alive after 120 days vs. 0% for the Abraxane® only group. Proof of concept for Acoustic Cluster Therapy has been demonstrated; ACT markedly increases the therapeutic efficacy of both paclitaxel and Abraxane® for treatment of human prostate adenocarcinoma in mice.

1. Introduction

Inadequate delivery into solid tumors is a well-recognized problem for a wide variety of chemotherapeutic agents, including small molecules, macromolecules such as monoclonal antibodies and cytokines, and larger constructs such as liposomes or other nanoparticles. Once administrated into the circulation, endothelial cells and other biological barriers restrict their passive extravasation into the tissue of the targeted pathology. Delivery of a systemically administrated agent to cells within solid tumors involves three processes: distribution through the vascular compartment, transport across the microvascular wall, and dispersion within the tumor interstitium [1,2]. However, for a number of drugs, the current, passive transvascular delivery paradigm, even when taking advantage of the Enhanced Permeability and Retention (EPR) effect or biochemical mechanisms, is inefficient and, together with poor penetration through the tumor interstitium, the drug often does not reach effective local concentrations with an inadequate therapeutic effect being the outcome. In combination with low therapeutic indexes, increasing the systemic dosages is not a viable strategy due to serious and wide spread adverse effects, overall limiting the clinical utility of a range of potent drugs.

For decades, scientists and the pharmaceutical industry have tried to find ways to enhance the efficacy of therapeutic agents with various approaches designed for specific delivery or enhanced uptake of the drug *within* the targeted pathology (i.e. targeted drug delivery). Successful strategies of this type may offer ways to increase the bioavailability and/or minimize systemic exposure, improving the therapeutic efficacy and reducing serious side effects [1–4]. Numerous drug carrier concepts, e.g. liposomes, micelles, dendrimers and nanoparticles have been employed, either to passively make use of the EPR effect, or in combination with surface ligands that actively promote accumulation in tumor tissue through biochemically affinity to specifically expressed target groups. In addition, active transport using human serum albumin has been exploited to target tumor tissue [5,6]; e.g. Abraxane® (nab-paclitaxel, paclitaxel bound to albumin).

However, even though huge resources have been spent on finding functional concepts for targeted drug delivery over the last two decades, and despite promising pre-clinical results for several of these, there has been very limited transition to drug products and clinical practice. In truth, the objective remains essentially unresolved in current standard of care medicinal therapy.

* Corresponding author at: Norwegian University of Science and Technology, 7491 Trondheim, Norge.
E-mail address: annemieke.wamel@ntnu.no (A. van Wamel).

http://dx.doi.org/10.1016/j.jconrel.2016.06.018
0168-3659/

In recent years, several concepts for ultrasound (US) mediated, targeted drug delivery have been investigated, some with quite encouraging results [7–12]. Many of these approaches explore the use of regular US contrast microbubbles such as Sonovue™ (Bracco Imaging S.p. A, Italy) or Optison™ (GE Healthcare AS, Norway) co-injected with various drug formulations. Insonation of the target pathology, containing microbubbles and drug in vascular compartments, leads to a variety of biomechanical effects that increase the permeability of the endothelial barrier leading to enhanced extravasation, distribution and uptake of drug molecules to target tissue [13–15]. Co-injection of Gemcitabine and Sonovue, with localized US insonation for enhanced drug uptake and therapeutic effect during treatment of pancreatic ductal adenocarcinoma is currently being explored in clinical trials [16]. A similar approach is being investigated for treatment of glioblastoma in humans [17,18]. Whereas various drug delivery approaches exploring the use of microbubbles have shown some promise, several issues hamper their effectiveness. Being small, the magnitude of the biomechanical work they can induce is relatively limited. In addition, being free flowing they display limited contact with the endothelial wall, reducing the level and range of the biomechanical effects [14]. Furthermore, microbubbles are typically cleared from vascular compartments within 2–3 min and, finally, to produce sufficient biomechanical work and effect levels, microbubbles often need a high US intensity that induces inertial cavitation, with ensuing safety issues.

Recently, a novel approach for US mediated, targeted drug delivery; Acoustic Cluster Therapy (ACT), has been suggested [19]. ACT exploits mechanisms that are related to those employed by regular microbubbles, but addresses important shortcomings of the latter. Details and attributes of the ACT formulation concept are described in [20,21]. In brief, the approach comprises co-administration of a drug together with a dispersion of microbubble/microdroplet clusters, followed by a two-step, local US activation and delivery enhancement procedure. US activation induces a liquid-to-gas phase shift of the microdroplet component and the formation of large (~25 μm) bubbles that transiently lodge in the targeted microvasculature, occluding blood flow. The subsequent US enhancement step induces controlled volume oscillations that lead to enhanced local permeability of the vasculature, allowing for improved extravasation and distribution of drug into the tumor tissue extracellular matrix. The ACT concept represents an unprecedented approach to targeted drug delivery that may improve significantly the efficacy of e.g. current chemotherapy regimen.

In our previous papers [20–22] we have described the basics of the ACT formulation and concept, shown the attributes of the large, activated bubbles in-vivo, and provided proof of principle for targeted, tumor specific uptake. In the current paper, we demonstrate proof of concept for this new treatment strategy by evaluating synergistic effects from combining ACT with paclitaxel and nab-paclitaxel (Abraxane®) for treatment of human prostate adenocarcinoma in mice.

2. Materials and methods

2.1. Mice and tumors

PC-3 human prostate adenocarcinoma cells (American Type Culture Collection, USA) were cultured in Dulbecco's modified Eagle medium (Life Technologies, USA) with 10% fetal bovine serum at 37 °C and 5% CO_2. Female athymic nude mice Balb/c nude mice (HsdOla: MF1-Foxn1nu, Envigo, Netherlands) were purchased at 6–8 week of age. The animals were housed in groups of five in individually ventilated cages (IVCs) (Model 1284 L, Techniplast, France). Mice were housed under conditions free of specific pathogens according to the recommendations set by the Federation for Laboratory Animal Science Associations [23]. The mice also had free access to food and sterile water and a controlled environment with temperatures kept between 19 and 22 °C and relative humidity between 50% and 60%. All experimental animal procedures were in compliance with protocols approved by the Norwegian National Animal Research Authorities. Before tumor implantation, mice were anesthetized with isoflurane, and a 50 μl suspension containing 3×10^6 PC-3 cells was slowly injected subcutaneously on the lateral aspect of the left hind leg between the hip and the knee. Tumors were allowed to grow for ~4 weeks until the volume of the tumor was between 100 and 200 mm^3. Anesthesia was induced by subcutaneous (s.c.) injection of midazolam (5 mg/kg)/fentanyl (0.05 mg/kg)/medetomidine (0.5 mg/kg) prior to each intervention described below. One hour after treatment, an antidote for sedation and anesthesia (atipamezole (2.5 mg/kg) and flumazenil (0.5 mg/kg)) was injected s.c. to wake up the mouse. Mice were kept for a minimum of 5 h in a recovery chamber after treatment. During all experiments the mouse body temperature was kept constant.

2.2. Test items

Test items were kindly provided by Phoenix Solution AS, Oslo, Norway. In brief, the ACT compound investigated consisted of a dispersion of microbubble/microdroplet clusters made from reconstituting the ultrasound contrast agent Sonazoid™ (GE Healthcare AS, Oslo, Norway) with 2 ml of perfluoromethylcyclopentane (PFMCP) microdroplets (3 μl/ml) stabilized with a distearoyl-phosphatidylcholine (DSCP) phospholipid membrane with 3% (mol/mol) stearylamine (SA), dispersed in 5 mM TRIS buffer. Further details on the ACT formulation are provided in [21].

Cytotoxic drugs investigated: Paclitaxel 6 mg/ml (Fresenius Kabi AB, Uppsala, Sweden) via *i.p.* injection and Abraxane™ 5 mg/ml (Celgene Ltd., Uxbridge, Great Britain) via i.v. injection.

2.3. Experimental set up

The experimental set up was as previously described [22]. In brief, total insonation duration was 5 min and 45 s. Initially, for activation (Activation US) of the clusters, the tumor was insonated for 45 s using a clinical broad-bandwidth phased array probe (Vscan, GE Healthcare AS, Oslo, Norway), with a Fc 2.5 MHz, 64 elements, frame rate of 20 Hz, and nominal mechanical index (MI) of 0.8 (Peak Negative Pressure, PNP, of 1.2 MPa). Actual MI was measured by a calibrated hydrophone to be approx. 0.4 (PNP of approx. 0.6 MPa) in the insonated tumor volume. Secondly, for the enhancement step (Enhancement US), after activation, the tumor tissue was insonated for 5 min with 500 kHz US at an MI of 0.2 (PNP of 0.14 MPa) using a custom made transducer (Imasonic SAS, Voray-sur-l'Ognon, France).

2.4. Groups, treatment regimens and responses

The study comprised eight groups, 7–10 animals in each, as detailed in Table 1. When the tumor size reached 100–200 mm^3 the mice were

Table 1
– Study design and treatment group.

Group	Test item	US procedure
Control	Saline	None (sham treatment)
Paclitaxel	12 mg Ptx/kg *i.p.*	45 s 2.25 MHz/MI 0.4 + 5 min 0.5 MHz/MI 0.2
Abraxane	12 mg Ptx/kg *i.v.*	45 s 2.25 MHz/MI 0.4 + 5 min 0.5 MHz/MI 0.2
ACT	3 × 5 mg pFMCP/kg *i.v.*	45 s 2.25 MHz/MI 0.4 + 5 min 0.5 MHz/MI 0.2
ACT + Paclitaxel	12 mg Ptx/kg *i.p.* + 3 × 5 mg pFMCP/kg *i.v.*	45 s 2.25 MHz/MI 0.4 + 5 min 0.5 MHz/MI 0.2
ACT + Abraxane	12 mg Ptx/kg *i.v.* + 3 × 5 mg pFMCP/kg *i.v.*	45 s 2.25 MHz/MI 0.4 + 5 min 0.5 MHz/MI 0.2
Sonazoid™ + Paclitaxel	12 mg Ptx/kg *i.p.* + 3 × 8 μl PFB/kg *i.v*	5 min 45 s 2.25 MHz/MI 0.4
Sonazoid™ + Abraxane	12 mg Ptx/kg *i.v.* + 3 × 8 μl PFB/kg *i.v*	5 min 45 s 2.25 MHz/MI 0.4

enrolled into the study. Treatment was given once a week for 4 weeks on days 0, 7, 14 and 21. Paclitaxel, given intraperitoneal (*i.p.*) 1 h before *i.v.* injection of ACT at a dose of 12 mg/kg, and Abraxane®, injected intravenously (*i.v.*) at a paclitaxel dose of 12 mg/kg, was administered immediately prior *i.v.* injection of ACT (5 mg pFMCP/kg) or Sonazoid™ (8 μl PFB/kg). For activation, immediately after ACT injection, the tumor was insonated for 45 s using the clinical VScan system. For enhancement, immediately after activation, the tumor tissue was insonated for 5 min, using the Imasonic, 500 kHz transducer. ACT and Sonazoid™ treatment were repeated three consecutive times at each cycle.

Animals were monitored for body weight and tumor size measured by caliper twice weekly for 120 days after study start. Animals were sacrificed when they reached the institutional ethical endpoint associated with tumor burden (tumor size > 15 mm or weight loss > 15%). A subset of 5 animals were found dead one after day treatment, in which case they were included in the tumor growth data until that time point. Compared to similar studies [24], the number of unexplained fall outs are low in number, and these deaths are not considered to be treatment related. In the ACT + ABR group one animal, although its tumor was very small, was sacrificed in week 5 because of a necrotic tail at the ABR injection site. This animal was therefore excluded from the survival data.

Only animals successfully undergoing procedures for the full 4 weeks were considered in the survival curves. The numbers of animal per group available for growth measurements were: control (9–9), Paclitaxel (9–9), Abraxane (10–9), ACT (9–8), ACT + PTX (10–7), ACT + ABR (10 − 10), Sonazoid + PTX (10–10), Sonazoid + ABR (9–9), where the range in numbers for a given group is the number of animals entering at week 0 and those completed the full 4 treatments.

For ethical reasons, in compliance with the Norwegian National Animal Research Authorities rule to reduce the number of research animals as much as possible, drug + US-only nor Sonazoid™ + US only groups were not included in the study as the US exposure levels are well below such that might cause bioeffects, even in the presence of microbubbles [25,26]. Similarly, Sonazoid nor ACT are, in the absence of US, not expected to affect tumor growth, and such groups were not included.

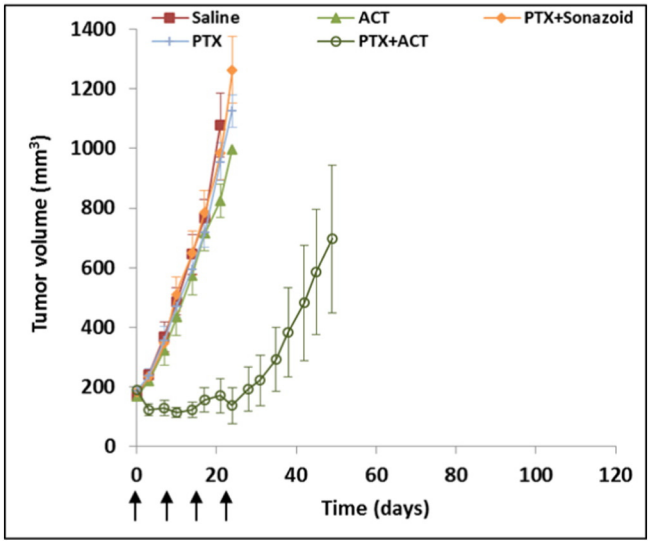

Fig. 1. Average tumor size in groups as detailed in the legend, vs. time. PTX = 12 mg paclitaxel/kg *i.p.*, ACT = 3 × 5 mg pFMCP/kg *i.v.*, Sonazoid = 3 × 8 μl PFB/kg *i.v.* Four weekly treatment points are designated by vertical arrows. Error bars represent standard error of the mean.

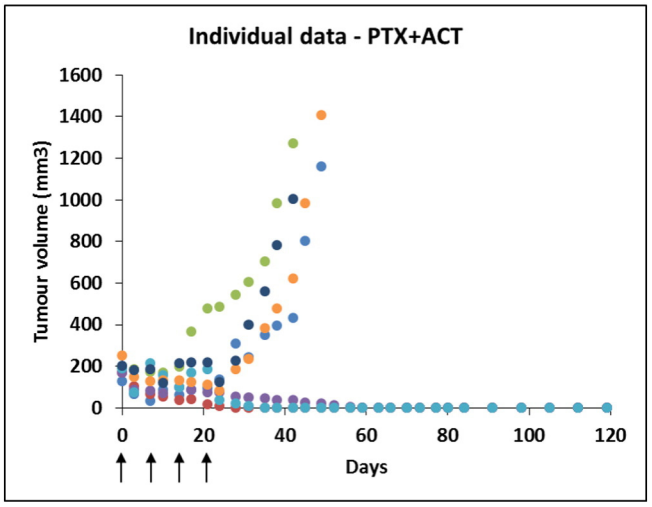

Fig. 2. Tumor size of individual animals in PTX + ACT group (cf. Fig. 1 for details), vs. time.

2.5. Statistical analysis

Results for average tumor volume are expressed as mean ± standard error. Statistical comparisons of tumor size at various time points were performed using a two-tailed, two sample Student's *t*-test assuming unequal variances. A p value <0.05 was considered statistically significant.

3. Results

3.1. Paclitaxel groups

Results for average tumor size in paclitaxel and control groups are shown in Fig. 1, results for tumor size of individual animals in the paclitaxel + ACT group are shown in Fig. 2 and results for survival are shown in Fig. 3.

As can be observed from Fig. 1, the paclitaxel and ACT monotherapies and the paclitaxel + Sonazoid™ groups did not display a significant effect on tumor growth rate vs. the saline control group. The paclitaxel + ACT group, however, shows a very strong inhibition of tumor growth rate, significantly different ($p = 0.0004$) from all other groups three days after the first treatment.

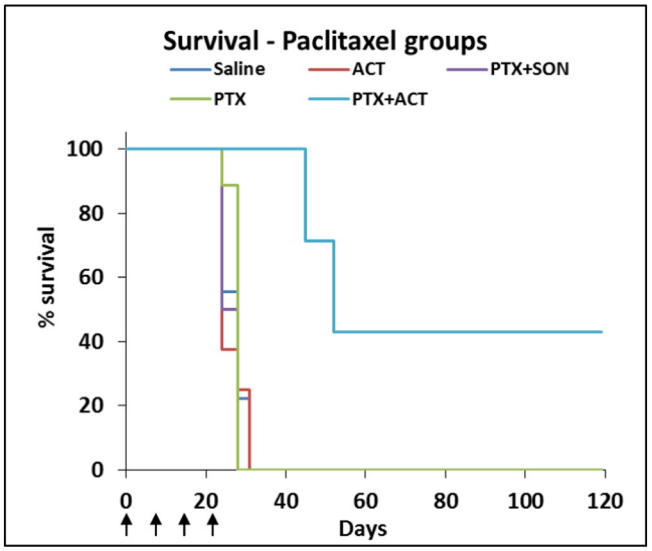

Fig. 3. Survival time curves paclitaxel treated animals.

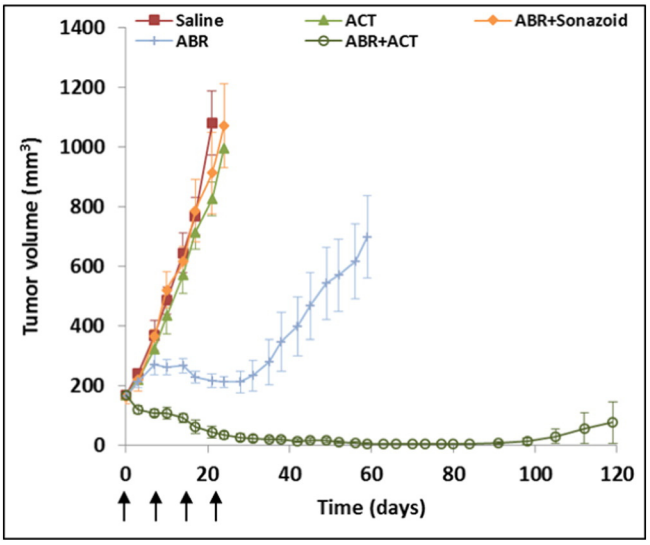

Fig. 4. Average tumor size in groups as detailed in the legend, vs. time. ABR = 12 mg paclitaxel/kg *i.p.*, ACT = 3 × 5 mg pFMCP/kg *i.v.*, Sonazoid = 3 × 8 μl PFB/kg *i.v.* Four weekly treatment points are designated by vertical arrows. Error bars represent standard error of the mean.

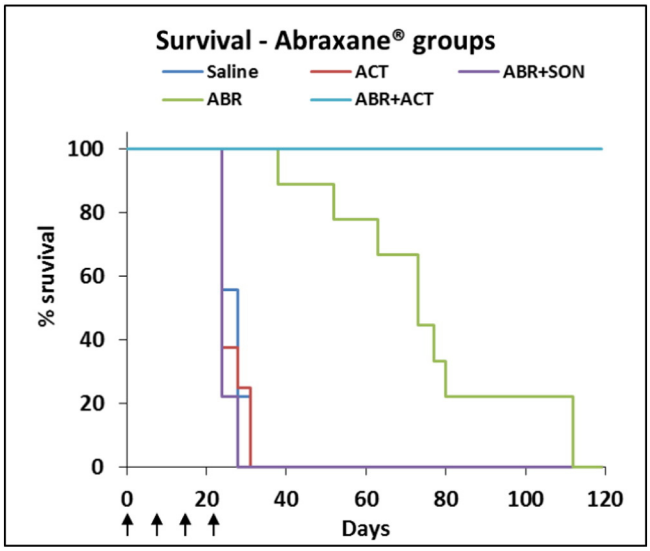

Fig. 6. Survival time curves Abraxane ® treated animals.

Four out of seven (58%) tumors started regrowing towards the end of or immediately after the end of the four-week treatment period. However, three tumors (42%) continued to regress to complete, stable remission after <60 days, which was kept for the duration of the study (Fig. 2). The median survival time was 52 days for the paclitaxel + ACT group vs. 28 days for the saline control group (Fig. 3).

3.2. Abraxane® groups

Results for average tumor size in Abraxane® and control groups are shown in Fig. 4, results for tumor size of individual animals in the Abraxane® and Abraxane® + ACT groups are shown in Fig. 5 and results for survival are shown in Fig. 6.

As can be observed from Fig. 4, the Abraxane® monotherapy displayed a marked reduction in tumor growth rate vs. the saline control group, with significant differences ($p = 0.0009$) from three days after the second treatment (day 10). The Abraxane® + ACT group, however, shows a very strong inhibition of tumor growth rate also vs. Abraxane® monotherapy, significantly different ($p = 0.002$) three days after the first treatment.

For the Abraxane® group, no tumors went to full remission and all tumors started regrowing between the end of the treatment regime and approx. 60 days. However, for the Abraxane® + ACT group, all tumors continued regression to complete remission after approx. 60 days and 6 out of 9 tumors (67%) were in stable, complete remission at end of study. Only one of 9 tumors displayed significant regrowth 120 days after study start. The median survival time was 72 days for the Abraxane® group vs. 28 days for the saline control group. Median survival time for the Abraxane® + ACT group could not be determined, as all animals were alive at end of study. Based on the results displayed in Fig. 6, however, it is estimated that the median survival time of this group would be at least 4 times that of the Abraxane® monotherapy group and possibly, indefinite.

The ACT monotherapy group did not display significant effects on tumor growth rate vs. the saline control. Remarkably, this was the case for the Abraxane® + Sonazoid group as well.

A summary of numeric responses for antitumor activity in all groups are given in Table 2.

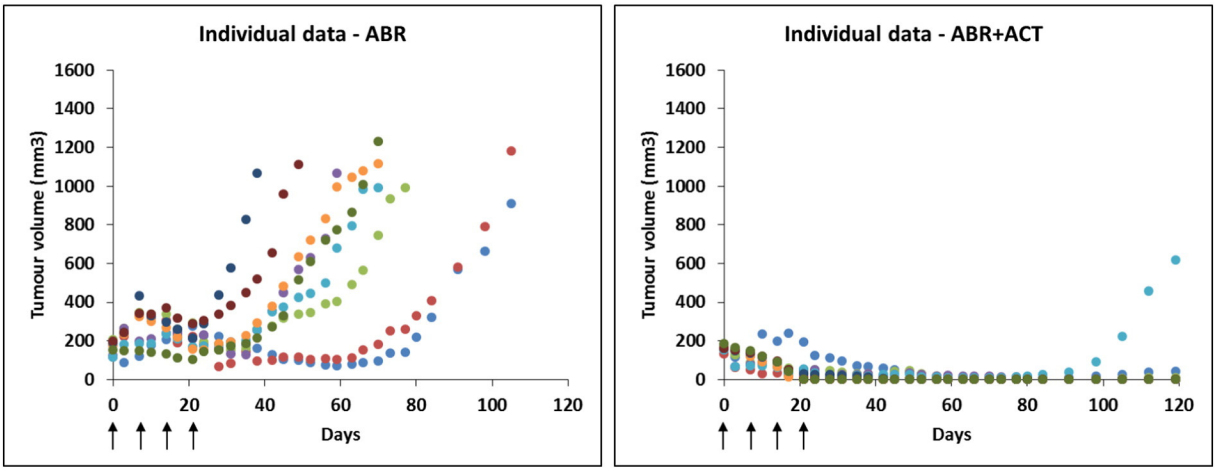

Fig. 5. Tumor size of individual animals in Abraxane® (left) and Abraxane® + ACT (right) groups (cf. Fig. 4 for details), vs. time.

Table 2
Antitumor activity of paclitaxel/Abraxane® in combination with ACT.

Treatment	N	TFS (%)[a]	Tumor doubling time (d), median (range)[b]
Control	9	0	8.2 (6.1–11.4)
PTX	9	0	8.6 (7.8–10.7)
ABR	9	0	23.4 (15.3–37.5)
ACT	8	0	9.4 (7.6–10.7)
ACT + PTX	7	42	Partial-responders 17.0 (15.4–19.8) Responders infinite
ACT + ABR	9	67	Infinite (64.9-infinite)
Sonazoid + PTX	10	0	7.9 (7.3–11.5)
Sonazoid + ABR	9	0	8.2 (5.6–9.2)

[a] Tumor free survivors after 120 days.
[b] Tumor doubling times were calculated using the equation $(t2 - t1)\ln 2 = \ln(V2/V1)$. t1 = first treatment day, t2 is last measurement day, V1 is tumor volume on first treatment day, V2 is tumor volume at last measurement day.

3.3. Tolerability

No treatment related weight changes (Fig. 7) were observed and no adverse events or signs of distress were observed during or immediately after treatment.

4. Discussion

The two therapeutic regimes studied, although in principal investigating the same active ingredient, are quite different. Giving paclitaxel *i.p.* will lead to a "slow release" of the drug into the vascular compartment, with ensuing low peak plasma concentrations and reduced bioavailability compared to an *i.v.* injection [27]. In essence, the 12 mg paclitaxel/kg given *i.p.* represents a sub-therapeutic regime – as observed. The motivation for investigating such a design was to mimic a clinically relevant infusion regime with regard to plasma pharmacokinetics (PK) and to show *one* of the potential aspects of ACT; increasing therapeutic efficacy of a low dose/low toxicity regime. Abraxane®, on the other hand, was given *i.v.* at a low, but clinically relevant dose. In this case, plasma concentrations reach therapeutic levels and this design allowed for demonstrating ACTs potential for increasing therapeutic efficacy of a Standard of Care regime. Clearly, the difference between the two formulations also influences the PK of the active substance. The regular formulation releases paclitaxel from Chremophor micelles in the plasma after administration, where almost all of the drug (approx. 95%) is quickly being bound to human serum albumin (HSA) protein molecules in the blood stream [28]. In Abraxane®, the paclitaxel is pre-bound to HSA. Whereas it is contained in a nano-particular structure upon injection, it immediately disintegrates to individual HSA-paclitaxel conjugates after administration [29]. It is the free paclitaxel that mediates the cytotoxic effect but the HSA-paclitaxel complex is in equilibrium with its unit components and acts like a reservoir of free drug. In summary, the active moieties are identical between the two regimes investigated, but the PKs are significantly different.

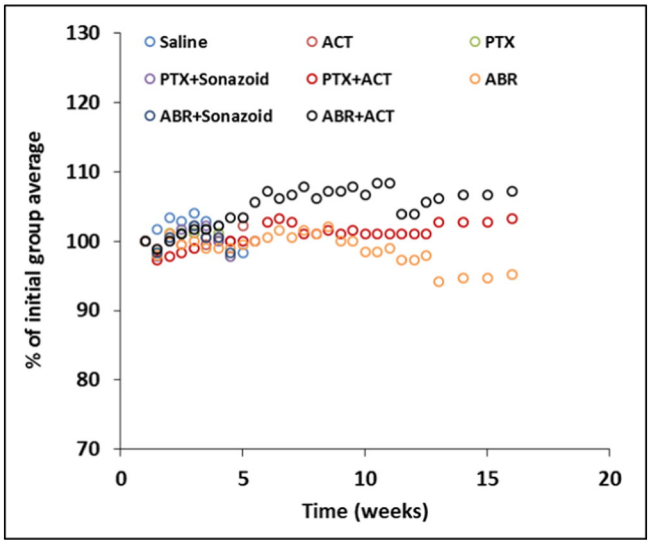

Fig. 7. Animal weights for all groups vs. time (average group weight at each monitoring point).

Our results clearly show the benefit of using ACT together with cytostatic drugs. Both in the "under dosed" paclitaxel group and with a clinically relevant dose of Abraxane®, we observe a very strong improvement in the anti-tumor activity of the drugs. This enhancement may be due to several possible mechanisms.

The use of small, regular contrast microbubbles such as Sonovue® or Optison® in combination with US has been shown to induce a series of biomechanical effects that may influence the extravasation, distribution, uptake and efficacy of co-administered drugs [13–15]. A bubble in the vascular compartment, oscillating in the sound field, will exert direct forces on the endothelial cells creating deformations. Such deformations may influence the vascular permeability, and the morphology and fluid dynamics in the interstitium. In addition, strong shear force fields are created which increase the convection of fluid in the vascular compartment, and may lead to enhancement of various transcellular uptake mechanisms. Compared to using regular contrast microbubbles, all of the above noted mechanisms should be strongly enhanced by the ACT concept. The ACT bubble is approx. 1000 times bigger by volume [20,21] and the level and range of the biomechanical effects induced should be orders of magnitude larger. In addition, the effects induced are strongly dependent upon the proximity of the bubble and the vessel wall [15]. Regular, free flowing microbubbles are typically moving and at a distance, whereas the ACT bubbles are for a period in constant close contact with the endothelium over a significant segment [21]. Furthermore, regular microbubbles are typically cleared from the vasculature 2–3 min after injection, whereas ACT bubbles deposits and stay for 5–10 min [22]. Also, we postulate that ACT, in addition to regular microbubble mechanisms, could influence the pressure gradient between the vascular compartment and the interstitium.

An oscillating ACT bubble will induce deformations of the vessel wall and the perivascular lining. This mechanical influence will pull the cells apart, generating or expanding fenestrations for enhanced permeability. Deformations of the endothelium can also result in disruptions in the interstitium and enhance the penetration of drug further into the tumor tissue. In essence, such mechanisms would represent an enhancement of the natural EPR effect. Targeting cancer cells using only EPR is not always a feasible strategy; the degree of tumor vascularization and porosity of tumor vessels can vary with the tumor type, status, and even throughout the same lesion [3,30–34]. As the ACT concept mechanically modulates the vascular permeability and the interstitium, heterogeneity of the EPR effect, effectively hindering sufficient tumor delivery, may be circumvented.

The oscillating ACT bubbles will also produce a significant shear stress and increased fluid convection (streaming patterns) in the vascular compartment. When endothelial cells are sensing shear stress they are stimulated to actively take up fluids and particles via endocytosis [35]. It is postulated that the transcellular transport of HSA-paclitaxel by endothelial cells via the GP-60 pathway [5,6] might also be enhanced due to these effects, resulting in a higher paclitaxel concentration in the tumor tissue.

Structures such as HSA bound paclitaxel are partly transported in the interstitium by convection; that is, they are carried by streaming of flowing fluid [36]. However, solid tumors show an increased interstitial fluid pressure (IFP), which forms a barrier to transcapillary transport [1, 37] and represents a significant obstacle in tumor treatment. Modification of the tumor interstitium might influence the IFP and facilitate the penetration of drugs into tumors [38–41]. In addition, when an ACT bubble deposits and occludes blood flow, the microvessel pressure

will increase upstream of the bubble, influencing the transcapillary pressure gradient in favor of enhanced extravasation.

Given *i.p.*, the 12 mg paclitaxel/kg dose did not reach a therapeutic effect level. From similar studies reported in literature [42], this is not surprising – apparently the plasma concentration of paclitaxel does not reach levels to induce significant tumor regression. However, the tumor responses observed when combining this regimen with ACT clearly demonstrate a strong therapeutic effect. Although all tumors responded to PTX + ACT treatment, the therapeutic effect became distinctively biomodal with time, with one group displaying full regrowth and one group regressing into stable, complete remission. Such effects are not uncommon. The prostate tumor xenograft used in this study is reported to be poorly vascularized [43], and will contain regions of hypoxia. Cells in hypoxic regions have a decreased supply of nutrients and although they are viable they are slowly proliferating or quiescent. Paclitaxel is more effective against proliferating than quiescent cells and slowly proliferating cells at increasing distances from tumor blood vessels are likely to be more resistant to therapy [34]. Furthermore, the transport of hydrophobic compounds like paclitaxel is retarded by hydrophobic elastin layers. When stuck to a lipid pool, the paclitaxel will stay where it is, resulting in a high concentration of drug close to the vessel wall and low concentrations further into the tumor tissue. Consequently, the slowly proliferating cells that are more resistant to paclitaxel also experience the lowest exposure to the drug. This might be the reason why paclitaxel treatment in our study was insufficient for a significant fraction of animals. Although we postulate that ACT increase the extravasation and the interstitial fluid flow in the tumor tissue, at low plasma concentrations it may not always be sufficient to push this lipid pool-binding agent towards all tumor cells. As it has been hypothesized that a single remaining cancerous cell can grow into a new tumor, a successful therapy must eliminate all residual malignant tumor cells to be curative. In our case, even at the low dose investigated, we observe a curative response in 42% of the tumors.

Given *i.v.*, the 12 mg paclitaxel/kg dose with Abraxane® show, as expected, a strong therapeutic effect. Again, data clearly demonstrate a strong increase in therapeutic effect, when combined with ACT. As noted, the peak plasma concentration of paclitaxel is likely to be orders of magnitude higher with Abraxane® given *i.v.* vs. regular paclitaxel given *i.p.* [27]. With the Abraxane® regime, the enhancement in extravasation and/or improvement of uptake and distribution induced by the combinatory ACT treatment is sufficient to lead to an almost total eradication of cancerous cells.

The reason for the complete depletion of the therapeutic effect of Abraxane® when combined with Sonazoid™ is not currently understood. However, in an effort to optimize biomechanical effects induced by Sonazoid™ microbubbles, the US Enhancement step for this group was performed by continuous insonation with 2.25 MHz and an MI of 0.4 for 5 min and 45 s. It is possible that this fairly strong and long regimen induce some kind of physiological response to shut down of the tumor vasculature, as has been reported elsewhere [24]. If so, this could prevent the drug penetrating tumor tissue and explain the lack of response in this group. Alternatively it could be due to some kind of physicochemical interaction e.g. Abraxane® adsorbing to the Sonazoid ™ microbubbles after injection, being carried rapidly to the liver and lowering the plasma concentration to sub-therapeutic levels. Studies are under way to elucidate possible causes for this observation.

The ACT concept has been shown to strongly increase the therapeutic efficacy of both low and clinically relevant doses of chemotherapeutic drugs. In a clinical setting, ACT would represent an image guided, localized therapy; the activated bubbles produce copious US backscatter in regular B-mode imaging [21], giving the operator a tool for confirmation of the spatial distribution and level of bubble deposition. By its nature, ACT would be indicated towards diseases where it is clinically meaningful to treat known, solid tumors with medicinal therapy. A number of relevant clinical scenarios exists; most cases where chemotherapy is used as a neoadjuvant or adjuvant before/after surgical resection, and several diseases where a known, solid and non-resectable tumor is the primary reason for morbidity and mortality. A particularly interesting indication for ACT could be treatment of locally advanced, non-resectable pancreatic adenocarcinoma. These tumors are quite easily imaged by US [44], and the current standard of care for this condition (gemcitabine, optionally in combination with nab-paclitaxel) shows very limited clinical utility and could gain significantly from a combination regime with ACT. Alternatively, locally advanced, hormone-refractory prostate adenocarcinoma, often treated with taxanes, could represent an interesting clinical indication for ACT, as could triple negative breast cancer treated with doxorubicin or liver metastases from colon rectal cancer.

Furthermore, ACT synergies are likely to be significant with a range of drugs; basically all that struggles with crossing the endothelial wall and penetrate the interstitium. As larger molecules/structures such as cytokines, monoclonal antibodies, and nano-drugs are particularly hindered by this biological barrier, ACT may prove a versatile instrument for novel, emerging drug therapies as well as existing chemotherapies.

Studies in orthotopic pancreatic adenocarcinoma models, including transgenic KRAS, treated with Abraxane® and/or gemcitabine are under way, as are triple negative breast cancer models treated with doxorubicin and Doxil™. Furthermore, mechanistic, pharmacokinetic and regulatory toxicity studies are planned for, and ACT is likely to enter into Phase I/IIa studies for treatment of non-resectable pancreatic cancer in 2018.

5. Conclusions

Proof of concept for Acoustic Cluster Therapy (ACT) has been demonstrated; ACT markedly increases the therapeutic efficacy of both paclitaxel and Abraxane® for treatment of human prostate adenocarcinoma in mice.

Acknowledgments

The authors thank Sigrid Berg, Sofie Snipstad, and Kristin Sæterbø for technical assistance. This work has been partially funded through the Norwegian Research Council grant number 228604.

References

[1] R.K. Jain, Barriers to drug delivery in solid tumors, Sci. Am. 271 (1994) 58–65.
[2] S.H. Jang, M.G. Wientjes, D. Lu, J.L. Au, Drug delivery and transport to solid tumors, Pharm. Res. 20 (2003) 1337–1350.
[3] F. Danhier, O. Feron, V. Preat, To exploit the tumor microenvironment: passive and active tumor targeting of nanocarriers for anti-cancer drug delivery, J. Control. Release 148 (2010) 135–146.
[4] J.A. Yared, K.H. Tkaczuk, Update on taxane development: new analogs and new formulations, Drug Des. Devel. Ther. 6 (2012) 371–384.
[5] A.M. Merlot, D.S. Kalinowski, D.R. Richardson, Unraveling the mysteries of serum albumin-more than just a serum protein, Front. Physiol. 5 (2014) 299.
[6] E. Miele, G.P. Spinelli, E. Miele, F. Tomao, S. Tomao, Albumin-bound formulation of paclitaxel (Abraxane ABI-007) in the treatment of breast cancer, Int. J. Nanomedicine 4 (2009) 99–105.
[7] J. Castle, M. Butts, A. Healey, K. Kent, M. Marino, S.B. Feinstein, Ultrasound-mediated targeted drug delivery: recent success and remaining challenges, Am. J. Physiol. Heart Circ. Physiol. 304 (2013) H350–H357.
[8] T.D. Khokhlova, Y. Haider, J.H. Hwang, Therapeutic potential of ultrasound microbubbles in gastrointestinal oncology: recent advances and future prospects, Ther. Adv. Gastroenterol. 8 (2015) 384–394.
[9] B.H. Lammertink, C. Bos, R. Deckers, G. Storm, C.T. Moonen, J.M. Escoffre, Sonochemotherapy: from bench to bedside, Front. Pharmacol. 6 (2015) 138.
[10] H.L. Liu, C.H. Fan, C.Y. Ting, C.K. Yeh, Combining microbubbles and ultrasound for drug delivery to brain tumors: current progress and overview, Theranostics 4 (2014) 432–444.
[11] K.H. Martin, P.A. Dayton, Current status and prospects for microbubbles in ultrasound theranostics, Wiley Interdiscip. Rev. Nanomed. Nanobiotechnol. 5 (2013) 329–345.
[12] J. Unga, M. Hashida, Ultrasound induced cancer immunotherapy, Adv. Drug Deliv. Rev. 72 (2014) 144–153.
[13] B. Geers, H. Dewitte, S.C. De Smedt, I. Lentacker, Crucial factors and emerging concepts in ultrasound-triggered drug delivery, J. Control. Release 164 (2012) 248–255.
[14] K. Kooiman, H.J. Vos, M. Versluis, N. de Jong, Acoustic behavior of microbubbles and implications for drug delivery, Adv. Drug Deliv. Rev. 72 (2014) 28–48.

[15] I. Lentacker, I. De Cock, R. Deckers, S.C. De Smedt, C.T. Moonen, Understanding ultrasound induced sonoporation: definitions and underlying mechanisms, Adv. Drug Deliv. Rev. 72 (2014) 49–64.
[16] S. Kotopoulis, G. Dimcevski, O.H. Gilja, D. Hoem, M. Postema, Treatment of human pancreatic cancer using combined ultrasound, microbubbles, and gemcitabine: a clinical case study, Med. Phys. 40 (2013) 072902.
[17] A. Carpentier, et al., Temporary Disruption of the Blood-Brain Barrier Using an Implantable Ultrasound System for Recurrent Glioblastoma Patients under IV Carboplatin Chemotherapy: Initial Phase 1/2a Clinical Trial Observations, Focused Ultrasound Foundation Symposium 2014, Washigtin, DC, USA 2014, p. 35.
[18] n.r.s.c. Nadia Norcia Radovini, World first: blood brain barrier opened non-invasively to deliver chemotherapy, in, Toronto, ON, http://sunnybrook.ca/media/item.asp?i=1351 2015.
[19] P.C. Sontum, A.J. Healey, S. Kvåle, in: P.S. AS (Ed.), Ultrasound Mediated Delivery of Drugs, 2014 (https://patentscope.wipo.int, Norway).
[20] A.J. Healey, P.C. Sontum, S. Kvale, M. Eriksen, R. Bendiksen, A. Tornes, J. Ostensen, Acoustic cluster therapy: in vitro and ex vivo measurement of activated bubble size distribution and temporal dynamics, Ultrasound Med. Biol. (2016).
[21] P. Sontum, S. Kvale, A.J. Healey, R. Skurtveit, R. Watanabe, M. Matsumura, J. Ostensen, Acoustic cluster therapy (ACT)–a novel concept for ultrasound mediated, targeted drug delivery, Int. J. Pharm. 495 (2015) 1019–1027.
[22] A. van Wamel, A. Healey, P.C. Sontum, S. Kvale, N. Bush, J. Bamber, C. de Lange Davies, Acoustic cluster therapy (ACT) - pre-clinical proof of principle for local drug delivery and enhanced uptake, J. Control. Release 224 (2016) 158–164.
[23] W. Nicklas, P. Baneux, R. Boot, T. Decelle, A.A. Deeny, M. Fumanelli, B. Illgen-Wilcke, Felasa, recommendations for the health monitoring of rodent and rabbit colonies in breeding and experimental units, Lab. Anim. 36 (2002) 20–42.
[24] D.E. Goertz, M. Todorova, O. Mortazavi, V. Agache, B. Chen, R. Karshafian, K. Hynynen, Antitumor effects of combining docetaxel (taxotere) with the antivascular action of ultrasound stimulated microbubbles, PLoS One 7 (2012), e52307.
[25] D.L. Miller, M.A. Averkiou, A.A. Brayman, E.C. Everbach, C.K. Holland, J.H. Wible Jr., J. Wu, Bioeffects considerations for diagnostic ultrasound contrast agents, J. Ultrasound Med. 27 (2008) 611–632 (quiz 633-616).
[26] T.R. Nelson, J.B. Fowlkes, J.S. Abramowicz, C.C. Church, Ultrasound biosafety considerations for the practicing sonographer and sonologist, J. Ultrasound Med. 28 (2009) 139–150.
[27] H. Gelderblom, J. Verweij, D.M. van Zomeren, D. Buijs, L. Ouwens, K. Nooter, G. Stoter, A. Sparreboom, Influence of Cremophor El on the bioavailability of intraperitoneal paclitaxel, Clin. Cancer Res. 8 (2002) 1237–1241.
[28] J. Liu, S. Liao, B. Diop-Frimpong, W. Chen, S. Goel, K. Naxerova, M. Ancukiewicz, Y. Boucher, R.K. Jain, L. Xu, TGF-beta blockade improves the distribution and efficacy of therapeutics in breast carcinoma by normalizing the tumor stroma, Proc. Natl. Acad. Sci. U. S. A. 109 (2012) 16618–16623.
[29] E. Brouwer, J. Verweij, P. De Bruijn, W.J. Loos, M. Pillay, D. Buijs, A. Sparreboom, Measurement of fraction unbound paclitaxel in human plasma, Drug Metab. Dispos. 28 (2000) 1141–1145.
[30] Y.H. Bae, Drug targeting and tumor heterogeneity, J. Control. Release 133 (2009) 2–3.
[31] S. Taurin, H. Nehoff, K. Greish, Anticancer nanomedicine and tumor vascular permeability; where is the missing link? J. Control. Release 164 (2012) 265–275.
[32] M.R. Junttila, F.J. de Sauvage, Influence of tumour micro-environment heterogeneity on therapeutic response, Nature 501 (2013) 346–354.
[33] P.L. Bedard, A.R. Hansen, M.J. Ratain, L.L. Siu, Tumour heterogeneity in the clinic, Nature 501 (2013) 355–364.
[34] O. Tredan, C.M. Galmarini, K. Patel, I.F. Tannock, Drug resistance and the solid tumor microenvironment, J. Natl. Cancer Inst. 99 (2007) 1441–1454.
[35] G. Apodaca, Modulation of membrane traffic by mechanical stimuli, Am. J. Physiol. Ren. Physiol. 282 (2002) F179–F190.
[36] B. Rippe, B. Haraldsson, Transport of macromolecules across microvascular walls: the two-pore theory, Physiol. Rev. 74 (1994) 163–219.
[37] A.D. Levin, N. Vukmirovic, C.W. Hwang, E.R. Edelman, Specific binding to intracellular proteins determines arterial transport properties for rapamycin and paclitaxel, Proc. Natl. Acad. Sci. U. S. A. 101 (2004) 9463–9467.
[38] C. de Lange Davies, L.M. Lundstrom, J. Frengen, L. Eikenes, S.O. Bruland, O. Kaalhus, M.H. Hjelstuen, C. Brekken, Radiation improves the distribution and uptake of liposomal doxorubicin (caelyx) in human osteosarcoma xenografts, Cancer Res. 64 (2004) 547–553.
[39] L. Eikenes, O.S. Bruland, C. Brekken, C. de Lange Davies, Collagenase increases the transcapillary pressure gradient and improves the uptake and distribution of monoclonal antibodies in human osteosarcoma xenografts, Cancer Res. 64 (2004) 4768–4773.
[40] A.I. Minchinton, I.F. Tannock, Drug penetration in solid tumours, Nat. Rev. Cancer 6 (2006) 583–592.
[41] P.A. Netti, D.A. Berk, M.A. Swartz, A.J. Grodzinsky, R.K. Jain, Role of extracellular matrix assembly in interstitial transport in solid tumors, Cancer Res. 60 (2000) 2497–2503.
[42] Z. Hui, Y. Xiao-ling, Q. Rui-fang, S. Fang-fan, S. Zheng-zhong, Inhibitory effects of curcumin in combination with paclitaxel on prostate cancer xenografted model, Prog. Mod. Biomed. 10 (2010) 823–827.
[43] K. Zhang, D.J. Waxman, Impact of tumor vascularity on responsiveness to antiangiogenesis in a prostate cancer stem cell-derived tumor model, Mol. Cancer Ther. 12 (2013) 787–798.
[44] G. Dimcevski, F.G. Erchinger, R. Havre, O.H. Gilja, Ultrasonography in diagnosing chronic pancreatitis: new aspects, World J. Gastroenterol. 19 (2013) 7247–7257.